Chinese Chemical Letters 34 (2023) 107590

Contents lists available at ScienceDirect

Chinese Chemical Letters

journal homepage: www.elsevier.com/locate/cclet

Solvent-mediated handedness inversed and amplified circularly polarized luminescence system based on camptothecin derivative

Xuan Wu[a,c], Ming Liu[b], Cheng Zheng[d], Yingying Wang[e], Yujing Zheng[b], Yuna Qian[a,c], Zhiyong Liao[d], Guoyong Fang[e,f], Jianliang Shen[a,b,c,*]

[a] Wenzhou Institute, University of Chinese Academy of Sciences, Wenzhou 325000, China
[b] School of Ophthalmology and Optometry, School of Biomedical Engineering, Wenzhou Medical University, Wenzhou 325035, China
[c] Oujiang Laboratory (Zhejiang Lab for Regenerative Medicine, Vision and Brain Health), Wenzhou 325001, China
[d] College of Life and Environmental Science, Wenzhou University, Wenzhou 325000, China
[e] College of Chemistry and Materials Engineering, Wenzhou University, Wenzhou 325000, China
[f] National Laboratory of Solid State Microstructures, Nanjing University, Nanjing 210093, China

ARTICLE INFO

Article history:
Received 15 April 2022
Revised 1 June 2022
Accepted 5 June 2022
Available online 10 June 2022

Keywords:
Circularly polarized luminescence
Chirality inversion and amplification
Solvent-incorporated self-assembly
Camptothecin derivative
Stimuli-responsiveness

ABSTRACT

To realize the handedness controllable circularly polarized luminescence (CPL) system remains challenging. Herein, the solvent-mediated CPL inversion and amplification systems were successfully constructed by camptothecin derivative (CPT-A). Due to the planar structure of *N,N*-dimethylformamide, it could co-assemble with CPT-A, resulting in the alteration of g_{lum} from −0.0082 to +0.0085 by increasing water content. While in the non-planar solvent (hexafluoroisopropanol), the g_{lum} was amplified to 0.034 with the increase in water content. Moreover, the CPT-A could react with the glutathione, resulting in the anticancer drug CPT to make it more toxic to the cancer cells. Overall, the handedness controllable CPL systems were realized by tuning the supramolecular self-assembly of a prodrug.

Recently, the circularly polarized luminescence (CPL) materials have attracted tremendous attention due to their potential application in the fields of 3D optical imaging, chiral sensing, and photoelectric devices [1–4]. Traditionally, the molecules with the intrinsic chirality could emit luminescence with only one kind of handedness. Therefore, to realize the alterable handedness of CPL seemed significant, which might provide diverse detection methods for sensing or bioimaging. In the past decades, many efforts have been devoted to realize the handedness inversion, such as the breaking of the molecular chiral balance, light-induced *cis-trans* isomerization, open-closed cyclization, or other external stimuli [5–8]. However, little effort has been engaged in the construction of CPL materials with the handedness inversion property [9,10]. The possible reason might be that the values of luminescence dissymmetry factor (g_{lum}) were usually low in the chiral molecules [11]. How to realize the amplification and inversion of CPL signal became an urgent issue in the construction of CPL materials with controllable handedness.

Supramolecular assembly, as a major aspect of supramolecular chemistry, has been widely explored, due to its potential application in functional materials [12–14]. Traditionally, the chiral signal could be remarkably amplified in the process of supramolecular assembly, which could improve the g_{lum} values of the CPL materials [15–21]. Moreover, under the external stimuli, the macroscopical or microscopical morphologies would be changed, resulting from the alteration in the supramolecular assembly manners [22–24]. Along with this line, it could be envisioned that the construction of stimuli-responsive supramolecular assembly with the CPL emission property might provide a possible way to realize the handedness-controllable CPL systems. Herein, an acrylate camptothecin derivative (CPT-A) was successfully synthesized. Due to the planar structure of CPT-A, there exited the strong $\pi\cdots\pi$ stacking interaction which played a vital role in its self-assembly process. To our delight, the CPT-A could self-assemble into different structures in different solvents, which exhibited different CPL emission behavior (Scheme 1). And the CPL signals of CPT-A exhibited remarkably amplification and inversion in these self-assembly processes. Meantime, the CPT-A could respond to the glutathione (GSH) in the cancer cells, resulting in the anticancer drug CPT to make it more toxic to the cancer cells.

* Corresponding author at: Wenzhou Institute, University of Chinese Academy of Sciences, Wenzhou 325000, China.
E-mail address: shenjl@wiucas.ac.cn (J. Shen).

https://doi.org/10.1016/j.cclet.2022.06.013
1001-8417/

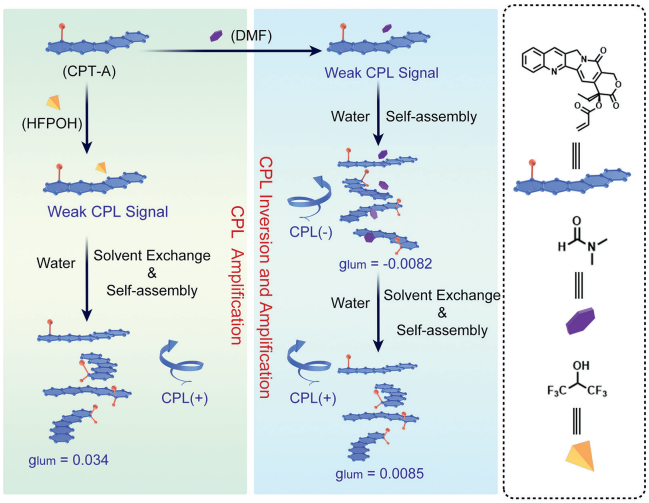

Scheme 1. Schematic illustration of self-assembly-mediated CPL inversion and amplification.

Camptothecin (CPT), as a Figureanti-cancer drug, has been extensively explored in drug delivery systems [25–27]. However, there are few pieces of research focused on its CPL property, even though its intrinsic fluorescence and chiral property. Herein, the CPT-A was successfully synthesized by the simple addition of the acryloyl chloride into the CPT solution. An interesting phenomenon could be observed in the characterization of CPT-A. The ^{1}H NMR spectra of CPT-A in different solvents were recorded and exhibited in Fig. S4 (Supporting information), from which it was observed the H_h splitted into two sets of peaks by using the $CDCl_3$ to replace DMSO-d_6, indicating the asymmetrical stacking of CPT-A could occur even in the moderate polar organic solvent. Moreover, the variant-concentration ^{1}H NMR spectroscopy also certificated the further assembly in $CDCl_3$. As shown in Fig. S5 (Supporting information), all the protons of the aromatic rings exhibited upfield-shift with the increase in the concentration.

The above phenomena also encouraged us to explore the solvent-mediated self-assembly behavior of CPT-A. Therefore, the ^{1}H NMR titration was further carried out by the addition of different solvents into $CDCl_3$ solution. Firstly, a strong polar solvent, *N,N*-dimethylformamide (DMF), was introduced, which could destroy the non-covalent interaction. However, an abnormal phenomenon could be observed. As shown in Fig. 1A, the addition of DMF up to 10 μL induced the downfield shift of H_g from 7.31 ppm to 7.42 ppm. Then the continual addition of DMF to the above solution resulted in the upfield shift to 7.36 ppm. The similar phenomena could also be observed from the proton H_e. To investigate the possible mechanism, the concentration-dependent NMR spectra of DMF in $CDCl_3$ were recorded and presented as Fig. S6 (Supporting information), which exhibited obvious upfield-shift of the protons on DMF with the increase in the volume of DMF, indicating the DMF could provide a shielding area for the compound around it. Therefore, the upfield-shift of protons on CPT-A might result from the formation of supramolecular complex with DMF, because the similar chemical-shift changes of DMF could be observed in this process (Fig. 1B). This phenomenon indicated the DMF might participate in the process of disaggregation then aggregation. However, different phenomena could be observed upon the addition of hexafluoroisopropanol (HFPOH). It was observed that with the gradual addition of HFPOH, the protons H_e and H_g shifted downfield obviously, and the C-H proton on the HFPOH exhibited no obvious shift (Figs. 1C and D). these different changes in the chemical-shifts might result from the different chemical structures of these two solvents, where the DMF was a planar structure, and HFPOH was a non-planar structure. And the planar DMF could form the stacking structure with CPT-A.

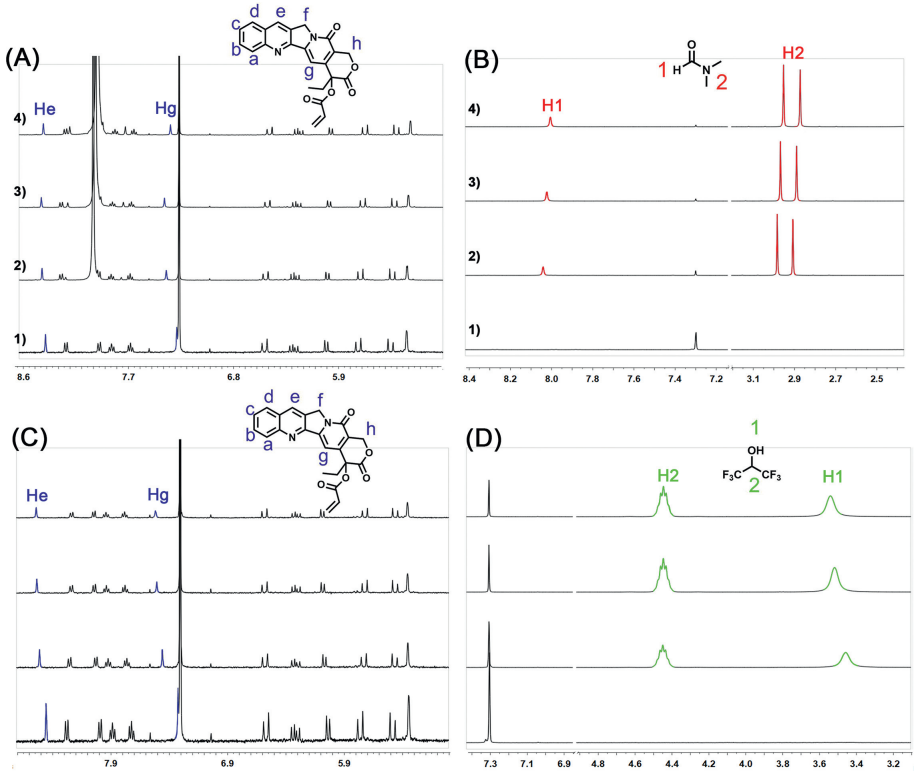

Fig. 1. Partial ^{1}H NMR spectra of CPT-A (400 MHz, $CDCl_3$, 298 K) after the addition of DMF (A, B) and HFPOH (C, D). (1) 500:0, (2) 495:5, (3) 490:10, and (4) 485:15 ($CDCl_3$:DMF, v/v).

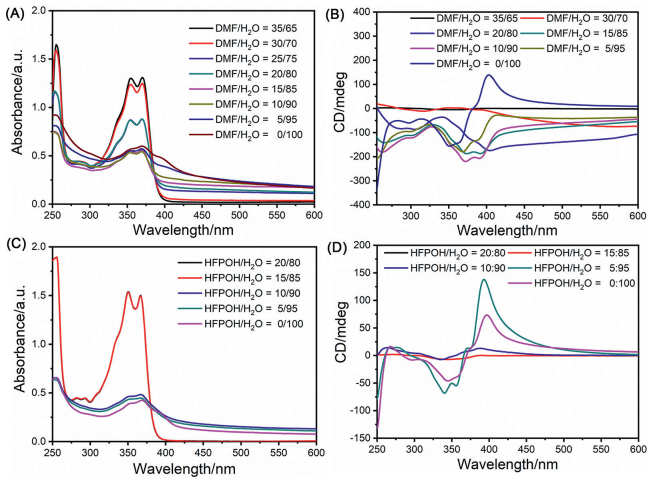

Fig. 2. UV-vis spectra of CPT-A in the mixed solution of DMF and H_2O (v/v) (A) and HFPOH and H_2O (v/v) (C). CD spectra of CPT-A in the mixed solution of DMF and H_2O (v/v) (B) and HFPOH and H_2O (v/v) (D). The 10 μL CPT-A solution in DMF ([CPT-A] = 20 mg/mL) was added to the above-mixed solution, and the final CPT-A concentration was determined to be 0.067 mg/mL.

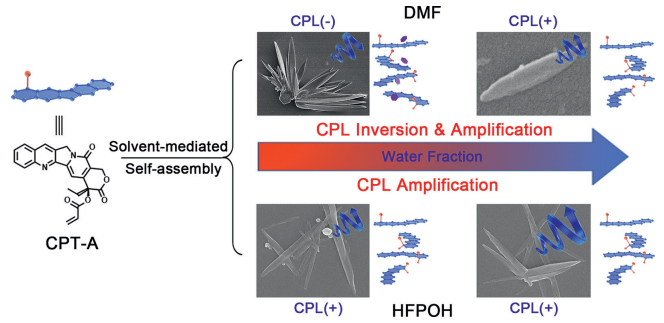

Scheme 2. Proposed solvent-mediated chirality inversion and amplification of CPT-A.

Due to the different influence resulting from DMF and HFPOH, the further self-assembly of CPT-A was investigated, as well as its assembly-induced chiral properties. Water, as a poor solvent of CPT-A, was chosen to investigate the solvent-mediated self-assembly and chiral properties. Firstly, their UV-vis spectra were recorded in the mixed solution with different water contents. As shown in Fig. 2A, with the increase of water content to 90% in the mixed solution of water and DMF, the characteristic absorption peaks of CPT-A at 353 and 369 nm decreased sharply, accompanied by the appearance of a new absorption peak at 403 nm. Moreover, the absorption intensities of these peaks increased with the continual increase in the water content. These processes were also certificated by the SEM images (Fig. S7 in Supporting information). From the obtained pictures, the original blocky structures transformed into regular petaloid structures. Finally, due to the solvent exchange between water and DMF, these petaloid structures collapsed into willow-leaf-shaped assembly. However, the addition of water in the HFPOH solution could lead to the continual decrease in the absorption peaks at 353 and 369 nm until the water content reached 95% (Fig. 2C). Then these peaks shifted to 356 nm, and 372 nm, accompanying with the appearance of a new absorption peak at 393 nm. And the SEM images indicated upon the gradual addition of water could result in the direct transformation from particles into willow-leaf-shaped assembly (Fig. S8 in Supporting information). The above results also indicated the DMF and HFPOH played vital roles in their respective self-assembly processes. Also the dynamic light scattering (DLS) spectroscopy was also employed to investigate these self-assembly processes. From the obtained profiles (Fig. S9 in Supporting information), it indicated with the gradual addition of water content, the sizes of formed assemblies increased, which was consistent with the obtained SEM images.

Encouraged by the solvent-induced self-assembly, the chiral properties were also investigated by the circular dichroism (CD) spectroscopy. The CD spectra of CPT-A in the mixed solution of DMF and water were depicted in Fig. 2B. The weak Cotton effect with negative peaks at 353 and 369 nm were observed in the mixed solution (H_2O:DMF, 35/65, v/v), which were assigned to the characteristic absorption peaks of CPT-A. And the strong Cotton effect with negative peaks at 392, 371, and 353 nm emerged with the gradual addition of water (10/90, H_2O:DMF, v/v), which might be resulted from self-assembly-induced chirality amplification. However, the continual increase in the water content led to the positive CD signals at 400 nm, and 379 nm, as well as the negative CD signals at 360 nm, and 347 nm. However, different phenomena could be observed in the system of HFPOH/water (Fig. 2D). In this system, a positive Cotton effect at 387 nm emerged, which was amplified and red-shifted to 397 nm with the continual increase in the water content. Moreover, the negative CD signals at 356 nm, and 344 nm were also amplified in these self-assembly processes. And the CD signal reached to the maximum at the water content of 95%. The difference in the solvent-mediated chirality change was consistent with the previous NMR spectroscopy and SEM images. From the previous results, it could be concluded the DMF was incorporated with CPT-A to form supramolecular complexes, which might be resulted from the planar structure of DMF. With the gradual addition of water, the co-assembly of DMF and CPT-A could be formed. However, due to solvent exchange between DMF and water, this co-assembly was collapsed, which led to the chirality inversion. However, due to the non-planar structure of HFPOH, the co-assembly could not be occurred, from which the chirality inversion could not be observed (Scheme 2).

To further certificate the above mentioned processes, the CD profiles of CPT-A were also obtained in the tetrahydrofuran (THF) and water systems. The similar phenomena with HFPOH could be observed (Fig. S11 in Supporting information), from which the amplification of CD signals could be detected. Moreover, the theoretical calculation was carried out to optimize the structures of CPT-A with DMF and HFPOH, respectively (Fig. S12 in Supporting information). From the optimized complexes between CPT-A and DMF/HFPOH (Fig. S12), different arrangement models could be observed. The stablest configuration between DMF and CPT-A was the parallel arrangement, which indicated the DMF was parallely placed on the CPT-A (Fig. S12A). However, in the HFPOH system, the stablest configuration was different, the HFPOH was arranged besides the CPT-A (Fig. S12C). Due to the planar structure of DMF, with the increse in the water content, another CPT-A molecule could arranged derectively on the DMF, thus resulting in the coassembly with DMF. However, in the HFPOH systems, the sandwich-like structure between the CPT-A and HFPOH could not be formed due to the arrangement between CPT-A and HFPOH. Even if the HFPOH was arranged above the CPT-A (Fig. S12B), the sandwich-like structure could not be formed, due to the difference between the chemical nature of HFPOH close to CPT-A and away from CPT-A. Therefore, with the increse in the water content, the HFPOH would be replaced directively, resulting in the assembly of CPT-A.

Therefore, due to the solvent-induced chirality amplification and inversion of CPT-A, its CPL properties were further investigated. Firstly, its fluorescence emission properties in different solutions were investigated. In the mixed solutions of DMF and water, the quench in the fluorescence emission at 430 nm could be observed with the increase in the water content (Fig. S13A in

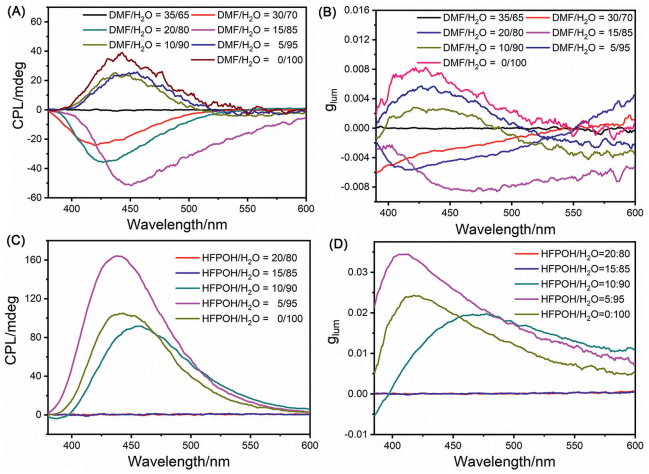

Fig. 3. (A) CPL spectra and (B) g_{lum} factor profiles of CPT-A in the mixed solution of DMF and H_2O (v/v). (C) CPL spectra and (D) g_{lum} factor profiles of CPT-A in the mixed solution of HFPOH and H_2O (v/v). The 10 μL CPT-A solution in DMF ([CPT-A] = 20 mg/mL) was added to the above mixed solution, and the final CPT-A concentration was determined to be 0.067 mg/mL.

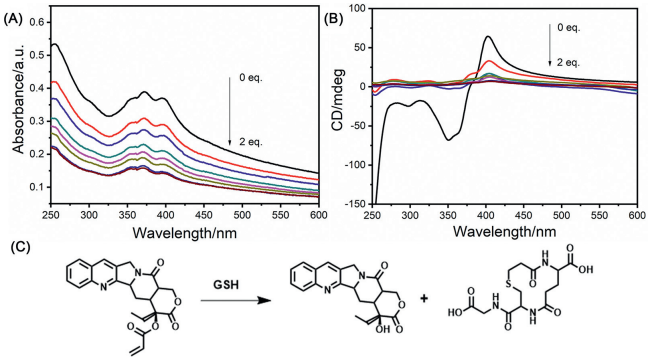

Fig. 4. (A) UV-vis spectra and (B) CD spectra of CPT-A after the addition of GSH. (C) Proposed reaction formula between CPT-A and GSH. The 10 μL CPT-A in DMF solution ([CPT-A] = 10 mg/mL) was added to water (3 mL), and the final CPT-A concentration was determined to be 0.033 mg/mL.

Supporting information). However, in the mixed solutions of HFPOH and water, the CPT-A exhibited different emission behavior (Fig. S13B in Supporting information), a new emission peak at 490 nm was observed, with the gradual addition of water, this emission peak decreased, and the emission peak at 420 nm increased until the water content reached 85%. After that, this emission peak decreased sharply, which was consistent with the ACQ nature of CPT. The different emission peaks in DMF and HFPOH systems (430 and 420 nm) also provided solid evidence for the different self-assembly patterns of CPT-A. Therefore, the self-assembly-induced CPL properties of CPT-A were further investigated.

Similar to the solvent-mediated amplification and inversion of CD signals, the CPL properties of CPT-A exhibited similar changes upon the increase in the water content (Fig. 3A). The negative CPL signal was observed after the addition of water to DMF solution, and its intensity increased until the water content reached 85%. After that this negative signal inversed, and a positive signal emerged. And in this process, the values of g_{lum} were changed from −0.0082 to +0.0085 (Fig. 3B). From the above results, the amplification and inversion of the CPL emission behavior of CPT-A could be finely realized by the solvents. Moreover, upon the addition of water to the HFPOH solution, a remarkable increase in the CPL intensity was observed (Fig. 3C), which showed the positive signals. And the signal reached the maximum at the water content of 95%, whose g_{lum} value was 0.034 (Fig. 3D). These phenomena were consistent with the solvent-induced amplification of CD signals.

Finally, the stability of CPT-A assembly was further investigated. Firstly, the concentration-dependent CD spectra were recorded. As shown in Figs. S15 and S16 (Supporting information), the intensity of characteristic CD signals exhibited a positive relationship with the CPT-A concentrations, indicating the formed assembly could be stably existed in the diluted solution. Moreover, this assembly also exhibited little responsiveness to the β-cyclodextrin (β-CD), which could encapsulate the CPT into its hydrophobic cavity (Fig. S18 in Supporting information) [28,29]. From both the UV-vis and CD spectra, little change occurred after the addition of β-CD. These results certificated the tight stacking between the CPT-A inhibited the formation host-guest complexation with β-CD.

What is more, its stability was also investigated in the presence of other chiral amino acids. As shown in Figs. S19A–C (Supporting information), the addition of amino acids (L-tryptophan, L-phenylalanine, and L-tyrosine) into the CPT-A solution could not result in the obvious changes in its absorption intensity, indicating these three kinds of amino acids could not affect the self-assembly behavior of CPT-A. However, in the presence of L-cysteine (Fig. S19D in Supporting information), the absorption intensity of CPT-A solution decreased sharply, which might be resulted from the reaction between the thiol group and the acrylate motif in the CPT-A [30]. This phenomenon enabled us to explore its potential application in the suppression of cancer cells.

Due to the over-expressed GSH in the cancer cells, its stimuli-behavior to the GSH was further investigated. From the UV-vis spectra (Fig. 4A), the addition of GSH could result in the a decrease in the characteristic absorption peaks of CPT-A assembly. Moreover, the CD spectra provided the same results (Fig. 4B), from which the characteristic CD signals decreased with the gradual addition of GSH. Moreover, the Tyndall effect was remarkably reduced after the addition of GSH (Fig. S21A in Supporting information), indicating the destruction of the formed assembly. And the SEM image also certificated this process, from which no regular assembly could be observed (Fig. S21B in Supporting information). Furthermore, the ESI-MS was employed to certificate the proposed mechanism, from which the peak at 360.3 (*m/z*) assigned to the byproduct could be found (Fig. S20 in Supporting information). Based on the above results, its toxicity on the cancer cells (MB49 cells) and normal cells (NIH3T3 cells) was investigated (Fig. S22 in Supporting information). Fortunately, after being co-incubated with CPT-A, the cell viability of MB49 cancer cells decreased sharply. Only 50% of cells remained alive at the concentration of 2 μmol/L, and 30% of alive cells could be detected at the concentration of 15 μmol/L. Moreover, due to relatively low GSH concentration in the NIH3T3 cells, the relatively higher cell viability could be detected in the same concentration. Therefore, it could be concluded the toxicity might be caused by the product from the reaction between CPT-A and GSH, in which the anticancer drug CPT could be obtained.

Herein, a acrylate modified CPT derivative (CPT-A) was successfully synthesized, which exhibited the different assembly behavior in different solvent systems. In the DMF system, due to the planar structure of DMF, the CPT-A and DMF could co-assemble into the ordered assembly with the gradual addition of water. However, the continual addition of water could destruct the CPT-A and DMF complex, resulting in the transformation from petaloid structures to willow-leaf-shaped assembly. Meantime, the CPL signals exhibited an amplification and inversion in the above assembly processes, whose g_{lum} values were changed from −0.0082 to +0.0085. However, in the nonplanar solvent HFPOH system, the addition of water could only result in the formation of a willow-leaf-shaped

assembly, and the amplification of the CPL signal, whose g_{lum} value could reach 0.034 in this process. Moreover, due to responsiveness to the GSH, the CPT could be afforded in the presence of GSH, which enabled it the potential application in the field of chiral drug delivery systems.

Declaration of competing interest

The authors declare no competing financial interest.

Acknowledgments

We thank the National Natural Science Foundation of China (No. 22101280), Wenzhou Medical University (No. KYYW201901), University of Chinese Academy of Science (Nos. WIBEZD2017001-03 and WIUCASQD2020005), and Zhejiang Provincial Natural Science Foundation (No. LQ20B020009) for financial support.

Supplementary materials

Supplementary material associated with this article can be found, in the online version, at doi:10.1016/j.cclet.2022.06.013.

References

[1] K. Dhbaibi, L. Favereau, M. Srebro-Hooper, et al., Angew. Chem. Int. Ed. 9 (2018) 735–742.
[2] M. Li, S.H. Li, D. Zhang, et al., Angew. Chem. Int. Ed. 57 (2018) 2889–2893.
[3] R. Sethy, J. Kumar, R. Métivier, et al., Angew. Chem. Int. Ed. 56 (2017) 15053–15057.
[4] G. Xia, L. Wang, H. Xia, et al., Chin. Chem. Lett. 33 (2022) 4253–4256.
[5] H. Wang, H.K. Bisoyi, B.X. Li, et al., Angew. Chem. Int. Ed. 59 (2020) 2684–2687.
[6] Z.G. Zheng, Y. Li, H.K. Bisoyi, et al., Nature 531 (2016) 352–356.
[7] E. Ohta, H. Sato, S. Ando, et al., Nat. Chem. 3 (2011) 68–73.
[8] K. Maeda, K. Shimomura, T. Ikai, et al., Macromolecules 50 (2017) 7801–7806.
[9] Q. Ye, F. Zheng, E. Zhang, et al., Chem. Sci. 11 (2020) 9989–9993.
[10] Y. Zhang, J. Wang, H. Chen, et al., Chin. Chem. Lett. 33 (2022) 2473–2476.
[11] X. Zhang, J. Yin, J. Yoon, Chem. Rev. 114 (2014) 4918–4959.
[12] K. Wang, J.H. Jordan, X.Y. Hu, L. Wang, Angew. Chem. Int. Ed. 59 (2020) 13712–13721.
[13] Y.M. Zhang, Y.H. Liu, Y. Liu, Adv. Mater. 32 (2020) 1806158.
[14] J. Zhou, L. Rao, G. Yu, et al., Chem. Soc. Rev. 50 (2021) 2839–2891.
[15] P. Xing, Y. Zhao, Acc. Chem. Res. 51 (2018) 2324–2334.
[16] L. Ji, Y. Sang, G. Ouyang, et al., Angew. Chem. Int. Ed. 58 (2019) 844–848.
[17] G. Park, H. Kim, H. Yang, et al., Chem. Sci. 10 (2019) 1294–1301.
[18] X. Yang, J. Han, Y. Wang, P. Duan, Chem. Sci. 10 (2019) 172–178.
[19] T. Zhao, J. Han, X. Jin, et al., Angew. Chem. Int. Ed. 58 (2019) 4978–4982.
[20] L. Yuan, Q.J. Ding, Z.L. Tu, et al., Chin. Chem. Lett. 33 (2022) 1459–1462.
[21] C. Wang, T. Jiang, X. Ma, Chin. Chem. Lett. 31 (2020) 2921–2924.
[22] W. Han, W. Xiang, Q. Li, et al., Chem. Soc. Rev. 50 (2021) 10025–10043.
[23] S.J.D. Lugger, S.J.A. Houben, Y. Foelen, et al., Chem. Rev. 122 (2022) 4946–4975.
[24] L. Zhang, H.X. Wang, S. Li, M. Liu, Chem. Soc. Rev. 49 (2020) 9095–9120.
[25] X. Liu, W. Shao, Y. Zheng, et al., Chem. Commun. 53 (2017) 8596–8599.
[26] S.Z.F. Phua, C. Xue, W.Q. Lim, et al., Chem. Mater. 31 (2019) 3349–3358.
[27] Y. Yang, Y.M. Zhang, D. Li, et al., Bioconjugate Chem. 27 (2016) 2834–2838.
[28] M. Ma, W. Shang, P. Xing, et al., Carbohydr. Res. 402 (2015) 208–214.
[29] A. Steffen, C. Thiele, S. Tietze, et al., Chem. Eur. J. 13 (2007) 6801–6809.
[30] Y. Yu, H. Xu, W. Zhang, et al., J. Photochem. Photobiol. Photobiol. A 346 (2017) 215–220.